Synthesis, Crystal Structure, and Magnetic Properties of (μ-Bipyrimidine)(cyanato)copper(II) and -(thiocyanato)copper(II) Complexes

Miguel Julve,*[1a] Michel Verdaguer,*[1b] Giovanni De Munno,[1c] José Antonio Real,[1a] and Giuseppe Bruno[1d]

Departament de Química Inorgànica, Facultat de Química de la Universitat de València, Dr. Moliner 50, 46100 Burjassot, València, Spain, Laboratoire de Chimie des Métaux de Transition, URA CNRS 419, Université Pierre et Marie Curie, 4 Place Jussieu, 75252 Paris, France, Dipartimento di Chimica, Università della Calabria, 87030 Arcavacata di Rende, Cosenza, Italy, and Dipartimento di Chimica Inorganica e Struttura Molecolare, Università di Messina, Messina, Italy

Received January 17, 1992

The synthesis, structure, and spectroscopic and magnetic properties of three 2,2′-bipyrimidine ($C_8H_6N_4$, bpm)-containing copper(II) complexes of formula $[Cu_2(bpm)(NCO)_4]_n$ (**1**), $[Cu(bpm)(NCS)_2]_n$ (**2**) and $[Cu_2(bpm)(NCS)_4]_n$ (**3**) are reported. Compounds **1** and **2** crystallize in the monoclinic system, space group $C2/c$ and Z = 4, with a = 19.486(1) Å, b = 7.527(1) Å, c = 15.252(1) Å, β = 137.8(2)°, and V = 1530.7(7) Å^3 for **1** and a = 11.543(1) Å, b = 13.948(2) Å, c = 7.818(1) Å, β = 93.26(1)°, and V = 1256.7(3) Å^3 for **2**, whereas compound **3** is orthorhombic, space group *Fddd*, with a = 12.811(1) Å, b = 22.473(1) Å, c = 24.259(1) Å, Z = 16, and V = 6983.9(7) Å^3. The copper environment in **1**–**3** is distorted octahedral. The structure of **1** consists of a 2D-array of copper(II) ions bridged by bis-bidentate bpm ligands and end-on and end to end cyanato groups. The structure of **2** is made up of 1D-chains of $[Cu(bpm)]^{2+}$ units linked by thiocyanato groups which act as asymmetrical end to end bridges. The structure of **3** consists of a 3D-network of copper(II) ions bridged by bis-bidentate bpm ligands and bis-unidentate end to end thiocyanato groups. The three compounds exhibit antiferromagnetic coupling, which is very weak in **2** (J = –0.6 cm^{-1}, $\hat{H} = -J \sum \hat{S}_i \hat{S}_{i+1}$) and strong in **1** and **3** (singlet–triplet energy gaps of –199 and –230 cm^{-1}, respectively). The efficiency of the bpm bridge in undergoing antiferromagnetic coupling between copper(II) ions which are separated by more than 5.5 Å is at the origin of the strong coupling observed in this series as revealed by a simple orbital model.

Introduction

The synthesis of alternating copper(II) chains and the study of their magnetic properties is one of the active fields in low-dimensional chemistry and physics.[2] The work in this area gave rise to new theoretical models[3] allowing to understand the thermodynamical properties of the chains and to new compounds with regularly alternating coupling constants J_i between the copper(II) ions[4] or more complex alternation situations.[5]

The general situation is the one with two antiferromagnetic J_1 and J_2 values with an alternation parameter $\alpha = J_1/J_2$, which is a possible model of a spin–Peierls distorted uniform chain. Examples of structurally alternating chains with J_i and J_{i+1} of different sign (ferro- and antiferromagnetic) are scarce, the best documented being the compound $Cu(hfac)_2(tempol)$[6] [hfac = (hexafluoroacetyl)acetonate anion; tempol = (4-hydroxy-2,2,6,6-tetramethylpiperidinyl)-*N*-oxy]. This kind of chain

$$\underbrace{M_{i-1}\ M_i}_{J_F}\ \underbrace{M_{i+1}\ M_{i+2}}_{J_{AF}}\ \underbrace{\quad}_{J_F}\ \underbrace{\quad}_{J_{AF}}$$

can be described as a chain of antiferromagnetically coupled S = 1 copper(II) triplets and can be of great interest to compare with the similar S = 1 nickel(II) chains designed to verify the Haldane conjecture.[7,8]

We undertook this study to obtain and to characterize such 1D-systems. 2,2′-Bipyrimidine, hereafter denoted as bpm, is well-known to bridge copper(II) ions in a bis-bidentate fashion. A (μ-bipyrimidine)copper(II) alternating chain is known containing μ-nitrato ions,[9] and alternating 2D-arrays are achieved when substituting the nitrate groups by chloro and bromo anions.[10] We thought that such a flexibility of the Cu(II)–bipyrimidine system, which leads also to mononuclear or binuclear species,[11] could be used to yield the expected chains with anions known to give rise to ferromagnetic interaction between two neighboring transition metal ions, such as azide, cyanate, and thiocyanate.[12]

We report here the results of our synthetic, spectroscopic, structural, and magnetic work on Cu(II)–bipyrimidine–X com-

(1) (a) Universitat de València. (b) Université Pierre et Marie Curie. (c) Università della Calabria. (d) Università di Messina.
(2) *Organic and Inorganic Low-Dimensional Crystalline Materials*; Delhaes, P., Drillon, M., Eds.; NATO ASI Series 168; Plenum: New York, 1987.
(3) Bonner, J. C. In *Magneto-Structural Correlations in Exchange Coupled Systems*; Willet, R. D., Gatteschi, D., Kahn, O., Eds.; NATO ASI Series; Reidel: Dordrecht; The Netherlands, 1985; p 157.
(4) Hatfield, W. E. In ref 3, p 555, and references therein.
(5) Landee, C. P. In ref 2, p 75, and references therein.
(6) (a) Bencini, A.; Benelli, C.; Gatteschi, D.; Zanchini, C. *J. Am. Chem. Soc.* **1984**, *106*, 5813. (b) Benelli, C.; Gatteschi, D.; Carnegie, D. W., Jr.; Carlin, R. L. *J. Am. Chem. Soc.* **1985**, *107*, 2560.
(7) (a) Haldane, F. D. M. *Phys. Lett.* **1983**, *A93*, 464. (b) Haldane, F. D. M. *Phys. Rev. Lett.* **1983**, *50*, 1153.
(8) (a) Renard, J. P.; Verdaguer, M.; Regnault, L. P.; Erkelens, W. A. C.; Rossat-Mignod, J.; Stirling, W. G. *Europhys. Lett.* **1987**, *3*, 945. (b) Renard, J. P.; Verdaguer, M.; Regnault, L. P.; Erkelens, W. A. C.; Rossat-Mignod, J.; Ribas, J.; Stirling, W. G.; Vettier, C. *J. Appl. Phys.* **1988**, *63*, 3538.
(9) De Munno, G.; Bruno, G. *Acta Crystallogr. Sect. C: Cryst. Struct. Commun.* **1984**, *C40*, 2030.
(10) Julve, M.; De Munno, G.; Bruno, G.; Verdaguer, M. *Inorg. Chem.* **1988**, *27*, 3160.
(11) (a) Castro, I.; Julve, M.; De Munno, G.; Bruno, G.; Real, J. A.; Lloret, F.; Faus, J. *J. Chem. Soc., Dalton Trans.* **1992**, 1739. (b) De Munno, G.; Bruno, G.; Julve, M.; Romeo, M. *Acta Crystallogr. Sect. C: Cryst. Struct. Commun.* **1990**, *C46*, 1828. (c) Matsubayashi, G.; Yosuhiro, Y.; Tanaka, T. *J. Chem. Soc., Dalton Trans.* **1988**, 2215. (d) Brewer, K. J.; Murphy, W. R.; Petersen, J. D. *Inorg. Chem.* **1987**, *26*, 3376. (e) Kaim, W.; Kohlmann, S. *Inorg. Chem.* **1987**, *26*, 68. (f) Brewer, G.; Sinn, E. *Inorg. Chem.* **1985**, *24*, 4580. (g) Ruminski, R. R. *Inorg. Chim. Acta* **1985**, *103*, 159. (h) Brewer, G.; Sinn, E. *Inorg. Chem.* **1984**, *23*, 2532. (i) Lanza, S. *Inorg. Chim. Acta* **1983**, *75*, 131. (j) Ruminski, R. R.; Petersen, J. D. *Inorg. Chem.* **1982**, *21*, 3706. (k) Petty, R. H.; Welch, B. R.; Wilson, L. J.; Bottomley, L. A.; Kadish, K. M. *J. Am. Chem. Soc.* **1980**, *102*, 611.

0020-1669/93/1332-0795$04.00/0

plexes (X = NCO, NCS): one complex with cyanate and two with thiocyanate of formulas $[Cu_2(bpm)(NCO)_4]_n$ (**1**), $[Cu(bpm)(NCS)_2]_n$ (**2**), and $[Cu_2(bpm)(NCS)_4]_n$ (**3**) have been synthesized and their structures solved. Our results demonstrate once more that molecular engineering and crystal engineering are always more difficult than first thought, particularly when the transition metal ions, like d^9 copper(II), are distorted by the Jahn–Teller effect.

Experimental Section

Materials. 2,2′-Bipyrimidine was purchased from Ventron (Ega Chimie) and used without purification. All other chemicals were reagent grade and they were used as received.

Synthesis. $[Cu_2(bpm)(NCO)_4]_n$ (1). This compound was obtained as a blue crystalline powder by adding an aqueous solution of sodium cyanate (4 mmol) to an aqueous ethanolic solution of copper(II) nitrate trihydrate (2 mmol) and 2,2′-bipyrimidine (1 mmol). The solid was washed with water and dried in vacuo over calcium chloride. The yield is quantitative. Single crystals of **1** were obtained as blue parallelepipeds by slow diffusion of the same solutions in an H-tube. Anal. Calcd for $C_{12}H_6N_8O_4Cu_2$ (**1**): C, 31.80; H, 1.32; N, 24.71. Found: 31.63, H, 1.21; N, 24.57.

$[Cu(bpm)(NCS)_2]_n$ (2). A dilute aqueous solution of potassium thiocyanate (250 mL, 0.5 mmol) was added to an aqueous solution of copper(II) nitrate trihydrate (0.5 mmol) and 2,2′-bipyrimidine (0.5 mmol) with heating and continuous stirring. The small amount of the brown precipitate of compound **3** was removed by filtration, and dark green prismatic single crystals of **2** were grown by slow evaporation of the resulting green solution. They were filtered off, washed with cold water, and stored under calcium chloride. Anal. Calcd for $C_{10}H_6N_6S_2Cu$ (**2**): C, 35.56; H, 1.78; N, 24.87; S, 18.98. Found: C, 35.54; H, 1.89; N, 24.86; S, 18.88.

$[Cu_2(bpm)(NCS)_4]_n$ (3). This compound was isolated as a maroon powder by adding an aqueous solution of potassium thiocyanate (4 mmol) to an aqueous solution of copper(II) nitrate trihydrate and 2,2′-bipyrimidine in a 4:2:1 molar ratio respectively. The product was filtered, washed with water and stored over calcium chloride. The yield is practically quantitative. Single crystals of **3** were obtained as maroon needles by slow diffusion of the foregoing solutions in an H-tube. Anal. Calcd for $C_{12}H_6N_8S_4Cu_2$ (**3**): C, 27.85; H, 1.16; N, 21.65; S, 24.78; Cu, 24.56. Found: C, 27.90; H, 1.67; N, 20.85; S, 23.75; Cu, 23.80.

Physical Techniques. Infrared spectra were recorded on a Pye Unicam SP 200 spectrophotometer as KBr pellets. The diffuse reflectance spectra were performed with a Perkin-Elmer Lambda 9 UV/vis/near-IR recording spectrometer for the compounds as Nujol mulls on filter paper.

Magnetic susceptibility measurements were carried out on polycrystalline samples in the 10–300 K temperature range for compounds **1** and **3** and in the 4.2–100 K range for compound **2** with a Faraday-type magnetometer, equipped with a helium flow cryostat. The apparatus was calibrated with mercury tetrakis(thiocyanato)cobaltate(II). Diamagnetic corrections to the susceptibility of complexes **1–3** were calculated from Pascal's constants[13] as -204×10^{-6} (**1**), -171×10^{-6} (**2**), and -244×10^{-6} (**3**) cm^3 mol^{-1}.

The X-band EPR spectra were recorded, both at room temperature and at 5 K, on polycrystalline samples of **1–3** with a Brüker ER 200 spectrometer equipped with a helium continuous flow cryostat.

X-ray Data Collection and Structure Refinement. Diffraction data were collected at room temperature on a CAD-4 Enraf-Nonius automatic diffractometer (**1** and **3**) and on a Siemens Stoe four-circle diffractometer (**2**) by using graphite-monochromated Mo Kα radiation (λ = 0.710 69 Å) (**1** and **2**) and graphite-monochromated Cu Kα radiation (λ = 1.541 80 Å) (**3**) and an ω–2θ scan technique. A 1.10 + 0.35 tan θ scan width was used for compounds **1** and **3**. Accurate unit-cell dimensions and crystal orientation matrices were obtained from least-squares refinement of 25 strong reflections in the $14 \le 2\theta \le 30°$ range for **1–3**. Details on crystal data, intensity collection, and structures refinement are summarized in Table I. All data were corrected for Lorentz and polarization effects. Absorption and extinction corrections were ignored.

Table I. Crystallographic Data for Compounds **1–3**

	1	**2**	**3**
chem formula	$C_{12}H_6N_8O_4Cu_2$	$C_{10}H_6N_6S_2Cu$	$C_{10}H_6N_8S_4Cu_2$
a, Å	19.846(1)	11.543(1)	12.811(1)
b, Å	7.527(1)	13.948(2)	22.473(1)
c, Å	15.252(1)	7.818(1)	24.259(1)
β, deg	137.8(2)	93.26(1)	90
V, Å^3	1530.7(7)	1256.7(3)	6983.9(7)
Z	4	4	16
fw	453.32	337.87	517.57
space group	$C2/c$	$C2/c$	$Fddd$
T, K	298	298	298
λ, Å	0.710 69	0.710 69	1.541 80
ρ_{calcd}, g cm^{-3}	1.967	1.785	1.969
μ, cm^{-1}	28.2	20.2	26.6
R^a	0.032	0.035	0.048
$R_w{}^b$	0.032	0.032	0.048

^{a} $R = \sum(|F_o| - |F_c|)/\sum|F_o|$. ^{b} $R_w = [\sum(|F_o| - |F_c|)^2/\sum w|F_o|^2]^{1/2}$.

The structures were solved by Patterson and Fourier methods, and refined by full-matrix least-squares calculations, with $\sum w(|F_o| - |F_c|)^2$ being minimized ($|F_o|$ and $|F_c|$ are the observed and calculated structure factors). All non-hydrogen atoms were refined anisotropically, whereas the hydrogen atoms, from the ΔF map, were refined with a common thermal parameter.

Of the 1386 measured reflections for **1**, 992 were unique with $I > 3\sigma(I)$, while these numbers were 1266 and 509 for **2**, and 1459 and 1292 for **3**. These data were used in the final refinement of the structural parameters to converge to final residuals R (R_w) of 0.032 (0.032) for **1**, 0.035 (0.032) for **2**, and 0.048 (0.048) for **3**. The weighting scheme used in the last refinement cycle was $w = 1.0565/(\sigma^2|F_o| + 0.000629F_c^2)$ for complex **2** whereas unit weights were used for complexes **1** and **3**. The anomalous dispersion corrections were taken from ref 15, atomic scattering factors for all non-hydrogen atoms from ref 16, and scattering factors for hydrogen atoms from ref 17. The values of the residual electron density were 0.53, 0.29, and 0.64 e Å^{-3} for complexes **1–3**, respectively. All calculations were performed with SHELX 76[14] and PARST[18] programs on a IBM 4341 computer from the Centro di Calcolo dell'Università di Messina and on a VAX/VMS computer from the Università della Calabria. Drawings were performed with SHELXTL-PLUS system[19] from Nicolet XRD Co on a micro-VAX II computer. Final fractional coordinates for non-hydrogen atoms of compounds **1–3** are listed in Tables II–IV, respectively. Main interatomic bond distances and angles are given in Tables V (**1**), VI (**2**), and VII (**3**). Crystallographic data (Table S1) (**1–3**), anisotropic temperature factors (Tables S2 (**1**), S3 (**2**), and S4 (**3**)), least-squares planes (Tables S5 (**1**), S6 (**2**), and S7 (**3**)), and nonessential bond distances and angles (Tables S8 (**1**), S9 (**2**) and S10 (**3**)) are available as supplementary material.

Results and Discussion

Description of the Structures. $[Cu_2(bpm)(NCO)_4]_n$ (1). The compound consists of $X_2Cu(bpm)CuX_2$ units (X = NCO) bridged by cyanate groups acting in asymmetrical end-on and end to end coordination modes (Figure 1). Cu atoms are in a distorted octahedral arrangement with a $[CuN_5O]$ chromophore. Four nitrogen atoms, two from bpm ligand and two from cyanate anions, occupy the equatorial positions, whereas the axial ones are filled by an oxygen and a nitrogen atom of other cyanate groups. A comparison of the R values for the end-on cyanate group assuming N coordination (R = 0.032) and O coordination (R = 0.040), and for the end to end fashion assuming equatorial N and axial

(12) (a) Charlot, M. F.; Kahn, O.; Chaillet, M.; Larrieu, C. *J. Am. Chem. Soc.* **1986**, *108*, 2574. (b) Cortés, R.; Arriortua, M. I.; Rojo, T.; Beltrán, D.; Debaerdemaeker, T. *Transition Met. Chem. (Weinheim, Ger.)* **1986**, *11*, 238. (c) Kahn, O., Boillot, M. L. In *Biological and Inorganic Copper Chemistry*; Karlin, K. D., Zubieta, J., Eds.; Adenine Press: New York, Vol. 2, 1985, p 187. (d) Kahn, O. *Comments Inorg. Chem.* **1984**, *3*, 105. (e) Duggan, D. M.; Hendrickson, D. N. *Inorg. Chem.* **1974**, *13*, 2929. (f) Ginsberg, A. P.; Martin, R. L.; Brookes, R. W.; Sherwood, R. C. *Inorg. Chem.* **1972**, *11*, 2884.
(13) Earshaw, A. *Introduction to Magnetochemistry*; Academic Press: London and New York, 1968.
(14) Sheldrick, G. M. SHELX 76, A Program for Crystal Structure Determination. University of Cambridge: Cambridge, England, 1976.
(15) *International Tables for X-Ray Crystallography*; Kynoch: Birmingham, England, 1974; Vol. IV, p 149.
(16) Reference 15, p 99.
(17) Stewart, R. F.; Davidson, E. R.; Simpson, W. T. *J. Chem. Phys.* **1965**, *42*, 3175.
(18) Nardelli, M. *Comput. Chem.* **1983**, *7*, 95.
(19) Sheldrick, G. M. SHELXTL-PLUS Crystallographic System, Version 2. Nicolet XRD Corp., Madison, WI, 1987.

Table II. Final Atomic Fractional Coordinates[a] and Equivalent Isotropic Displacement Parameters[b] for Compound **1**

atom	*x/a*	*y/b*	*z/c*	U_{eq}, Å^2
Cu	0.5793(1)	0.3387(1)	0.5717(1)	0.027(1)
N(1)	0.5849(3)	0.1129(5)	0.6527(3)	0.024(2)
N(2)	0.4774(3)	0.1821(5)	0.4061(3)	0.025(2)
N(3)	0.5564(3)	0.5374(5)	0.4690(4)	0.038(2)
N(4)	0.6944(4)	0.4376(6)	0.7402(5)	0.042(3)
C(1)	0.6377(4)	0.0782(7)	0.7765(5)	0.031(3)
C(2)	0.5293(3)	−0.0195(6)	0.5671(4)	0.024(2)
C(3)	0.4243(4)	0.2150(7)	0.2816(5)	0.032(3)
C(4)	0.6339(4)	−0.0861(7)	0.8124(5)	0.036(3)
C(5)	0.7511(4)	0.5248(7)	0.8312(5)	0.039(3)
C(6)	0.5942(5)	0.5828(9)	0.4424(6)	0.052(4)
O(1)	0.8102(3)	0.6194(6)	0.9260(4)	0.063(3)
O(2)	0.6328(5)	0.6220(13)	0.4121(7)	0.151(7)
H(1)	0.670(4)	0.166(7)	0.832(5)	0.060[c]
H(2)	0.421(4)	0.330(7)	0.262(5)	0.060[c]
H(3)	0.668(4)	−0.112(6)	0.903(5)	0.060[c]

[a] Estimated standard deviations in the last significant digits are given in parentheses. [b] U_{eq} is defined as one-third of the trace of the orthogonalized U_{ij} tensor. [c] Isotropic temperature factor.

Table III. Final Atomic Fractional Coordinates[a] and Equivalent Isotropic Displacement Parameters[b] for Compound **2**

atom	*x/a*	*y/b*	*z/c*	U_{eq}, Å^2
Cu	0.5000	0.1298(1)	0.2500	0.041(1)
S	0.2982(1)	−0.1331(1)	0.4569(1)	0.048(1)
N(1)	0.4463(4)	0.2398(4)	0.3915(7)	0.030(3)
N(2)	0.4455(5)	0.4099(4)	0.4057(8)	0.040(3)
N(3)	0.4029(5)	0.0355(4)	0.3553(8)	0.045(4)
C(1)	0.3964(6)	0.2349(6)	0.5417(10)	0.043(5)
C(2)	0.3701(6)	0.3173(6)	0.6280(10)	0.045(5)
C(3)	0.3957(7)	0.4032(5)	0.5539(10)	0.047(5)
C(4)	0.4704(5)	0.3286(5)	0.3312(8)	0.017(4)
C(5)	0.3597	0.0336(5)	0.8974(9)	0.019(5)
H(1)	0.381(6)	0.181(5)	0.589(9)	0.060[c]
H(2)	0.328(6)	0.319(5)	0.726(9)	0.060[c]
H(3)	0.383(5)	0.459(5)	0.608(9)	0.060[c]

[a] Estimated standard deviations in the last significant digits are given in parentheses. [b] U_{eq} is defined as one third of the trace of the orthogonalized U_{ij} tensor. [c] Isotropic temperature factor.

Table IV. Final Atomic Fractional Coordinates[a] and Equivalent Isotropic Displacement Parameters[b] for Compound **3**

atom	*x/a*	*y/b*	*z/c*	U_{eq}, Å^2
Cu(1)	0.6250	0.1250	1.0118(1)	0.032(1)
Cu(2)	0.3750	0.2525(1)	0.8750	0.036(1)
S(1)	0.3963(1)	0.1179(1)	1.0232(1)	0.036(1)
S(2)	0.6027(1)	0.2639(1)	0.8679(1)	0.036(1)
N(1)	0.6244(4)	0.0658(2)	1.0762(2)	0.027(2)
N(2)	0.3748(4)	0.3225(2)	0.8203(2)	0.029(2)
N(3)	0.6273(5)	0.1877(2)	0.9579(2)	0.044(3)
N(4)	0.3728(5)	0.1948(2)	0.9335(3)	0.053(4)
C(1)	0.6250	0.0925(3)	1.1250	0.023(4)
C(2)	0.6242(5)	0.0064(2)	1.0759(2)	0.033(3)
C(3)	0.6250	−0.0258(3)	1.1250	0.037(5)
C(4)	0.6158(5)	0.2189(2)	0.9197(2)	0.031(3)
C(5)	0.3841(5)	0.1624(2)	0.9706(3)	0.033(3)
C(6)	0.3748(6)	0.3229(3)	0.7641(2)	0.036(3)
C(7)	0.3750	0.3750	0.7366(3)	0.039(5)
C(8)	0.3750	0.3750	0.8446(3)	0.025(4)
H(1)	0.625(7)	−0.012(3)	1.051(3)	0.060[c]
H(2)	0.625	−0.060(5)	1.125	0.060[c]
H(3)	0.372(7)	0.293(4)	0.749(3)	0.060[c]
H(4)	0.375	0.375	0.699(5)	0.060[c]

[a] Estimated standard deviations in the last significant digits are given in parentheses. [b] U_{eq} is defined as one third of the trace of the orthogonalized U_{ij} tensor. [c] Isotropic temperature factor.

O (R = 0.032) and axial N and equatorial O coordination (R = 0.038) enabled us to conclude that the end-on cyanato is N-coordinated and that the end to end cyanato is bonded to through the N atom in the equatorial position to copper.

The present compound is isostructural to $[Cu_2(bpm)(NO_3)_4]_n$, whose structure was already reported.[9] As in the nitrate compound, there are two copper atoms bridged by two cyanato groups which act in an end-on fashion by means of N atoms (O atoms of nitrate groups act as bridges in the nitrate compound), the Cu–N distances being 1.961(4) and 2.456(7) Å for the N(3) and N(3b) atoms in the equatorial and axial positions respectively. The cyanato bridges lead complex **1** to adopt a polymeric array similar to that displayed by the nitrate compound. As in the latter case, the bpm bridging planes of different units which are bridged by NCO groups are parallel (see Figure 2), but at a

Table V. Selected Bond Lengths (Å) and Interbond Angles (deg) for Compound **1**[a]

Distances			
Cu–N(1)	2.054(4)	Cu–N(4)	1.919(4)
Cu–N(2)	2.072(4)	Cu–N(3b)	2.456(7)
Cu–N(3)	1.961(4)	Cu–O(1c)	2.724(7)
Angles			
N(1)–Cu–N(2)	80.3(1)	N(4)–Cu–O(1c)	94.0(2)
N(1)–Cu–N(3)	171.4(2)	N(4)–Cu–N(3b)	100.7(2)
N(1)–Cu–N(4)	92.0(2)	O(1c)–Cu–N(3b)	162.8(1)
N(1)–Cu–O(1c)	78.9(2)	Cu–N(1)–C(1)	130.2(3)
N(1)–Cu–N(3b)	91.6(2)	Cu–N(1)–C(2)	113.3(3)
N(2)–Cu–N(3)	91.2(2)	C(3)–N(2)–Cu	130.7(3)
N(2)–Cu–N(4)	166.5(2)	Cu–O(1c)–C(5c)	115.4(5)
N(2)–Cu–O(1c)	73.8(1)	Cu–N(3)–C(6)	113.7(5)
N(2)–Cu–N(3b)	90.6(2)	Cu–N(3)–Cu(b)	93.1(2)
N(3)–Cu–N(4)	96.6(2)	C(6)–N(3)–Cu(b)	133.2(4)
N(3)–Cu–O(1c)	110.4(2)	Cu–N(4)–C(5)	166.6(5)
N(3)–Cu–N(3b)	86.9(2)		

[a] Symmetry code: (a) $1-x, -y, 1-z$; (b) $1-x, 1-y, 1-z$; (c) $^3/_2 - x, -^1/_2 + y, ^3/_2 - z$.

Table VI. Selected Bond Lengths (Å) and Interbond Angles (deg) for Compound **2**[a]

Distances			
Cu–N(1)	2.009(6)	Cu–S(b)	3.174(2)
Cu–N(3)	1.941(6)		
Angles			
N(1)–Cu–N(1a)	80.5(2)	N(3a)–Cu–S(c)	97.0(2)
N(1)–Cu–N(3a)	162.6(2)	S(b)–Cu–S(c)	178.3(2)
N(1)–Cu–N(3)	92.6(2)	C(5)–S–Cu(b)	83.1(2)
N(1)–Cu–S(b)	80.1(1)	Cu–N(1)–C(1)	127.3(5)
N(1)–Cu–S(c)	98.6(1)	Cu(1)–N(1)–C(4)	115.4(4)
N(3a)–Cu–N(3)	94.7(2)	Cu–N(3)–C(5)	165.0(6)
N(3a)–Cu–S(b)	84.2(2)		

[a] Symmetry code: (a) $1-x, y, ^1/_2 - z$; (b) $1-x, -y, 1-z$; (c) $x, -y, -^1/_2 + z$.

Table VII. Selected Bond Lengths (Å) and Interbond Angles (deg) for Compound **3**[a]

Distances			
Cu(1)–S(1)	2.947(1)	Cu(2)–S(2)	2.933(1)
Cu(1)–N(1)	2.052(5)	Cu(2)–N(2)	2.060(5)
Cu(1)–N(3)	1.921(5)	Cu(2)–N(4)	1.923(6)
Angles			
N(1)–Cu(1)–N(1a)	80.8(2)	N(2)–Cu(2)–N(2d)	80.3(2)
N(1)–Cu(1)–N(3)	173.3(2)	N(2)–Cu(2)–N(4)	172.5(2)
N(1)–Cu(1)–N(3a)	92.4(2)	N(2)–Cu(2)–N(4d)	92.3(2)
N(1)–Cu(1)–S(1)	83.7(2)	N(2)–Cu(2)–S(2)	84.1(1)
N(1)–Cu(1)–S(1a)	88.1(1)	N(2)–C(2)–S(2d)	88.2(1)
N(1a)–Cu(1)–N(3)	92.4(2)	N(2d)–Cu(2)–N(4)	92.3(3)
N(3)–Cu(1)–N(3a)	94.3(2)	N(4)–Cu(2)–N(4d)	95.2(2)
N(3)–Cu(1)–S(1)	96.8(2)	N(3)–Cu(1)–S(1a)	90.5(1)
N(4)–Cu(2)–S(2d)	90.1(4)	N(4)–Cu(2)–S(2)	96.7(2)
S(1)–Cu(1)–S(1a)	169.2(1)	S(2)–Cu(2)–S(2d)	170.0(4)
Cu(1)–N(1)–C(1)	112.7(4)	Cu(2)–N(2)–C(8)	113.3(4)
Cu(1)–N(1)–C(2)	130.2(4)	Cu(2)–N(2)–C(6)	130.5(4)
Cu(1)–N(3)–C(4)	167.1(5)	Cu(2)–N(4)–C(5)	171.3(6)

[a] Symmetry code: (a) $^5/_4 - x, ^1/_4 - y, z$; (b) $^5/_4 - x, y, ^9/_4 - z$; (d) $^3/_4 - x, y, ^7/_4 - z$; (f) $^3/_4 - x, ^3/_4 - y, z$.

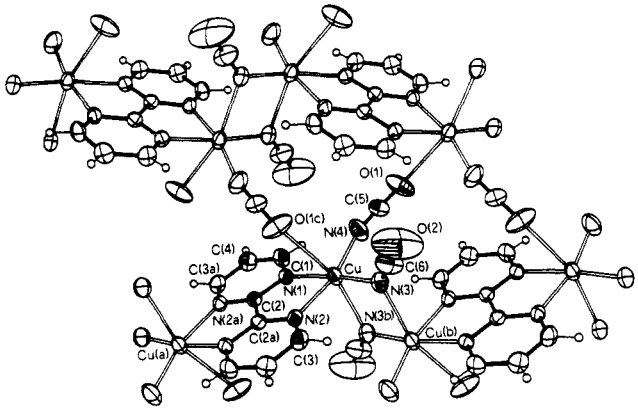

Figure 1. (a) ORTEP view of the $[Cu_2(bpm)(NCO)_4]_n$ complex (**1**) with the atom numbering scheme. Thermal ellipsoids are plotted at the 50% probability level. Shaded ellipsoids represent the atoms of the asymmetric unit. All hydrogen atoms are drawn with uniform isotropic thermal parameters.

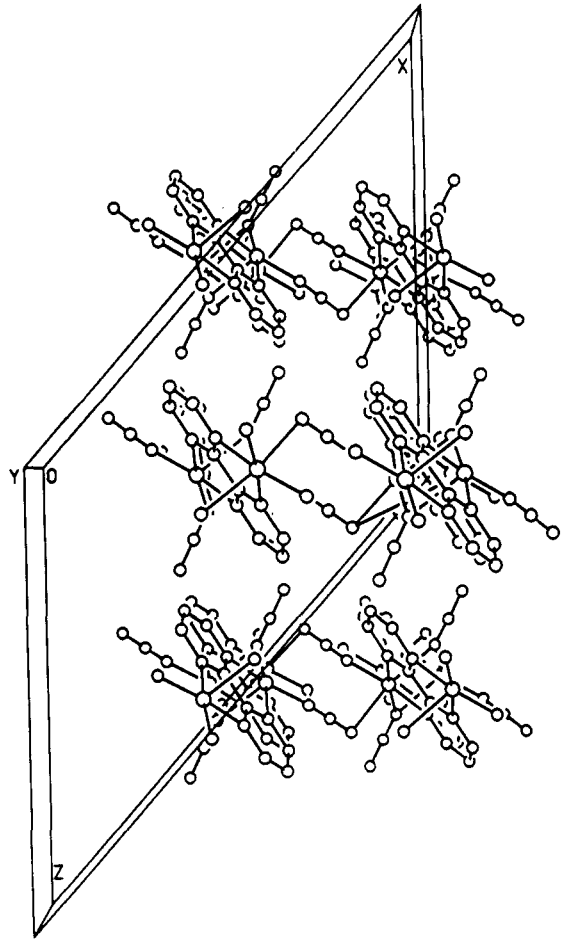

Figure 2. View of the cell of complex **1** along the *b*-axis (the *c*-axis is vertical) showing the arrangement of different planes in the crystal. Atoms are plotted with arbitrary atomic radii. Hydrogen atoms have been omitted for clarity.

distance of 2.210(1) Å instead of 1.946 Å found for the nitrate compound. The Cu···Cu(b) distance is 3.418(1) Å. This is related to the different angle around the N atom of the end-on cyanate groups, which is 93.1(2)° in **1**, while the Cu–O–Cu′ angle in the nitrate compound is 106.3(1)°. Although both cyanate and nitrate compounds are isostructural, the former one shows a different arrangement. The mean difference is due to the presence of end to end NCO bridging ligands, which coordinate to copper through the N atom in the equatorial position and through the O atom in the axial one (Cu–N(4) and Cu–O(1c) distances are 1.919(4) and 2.724(7) Å, respectively). Every copper atom is, therefore,

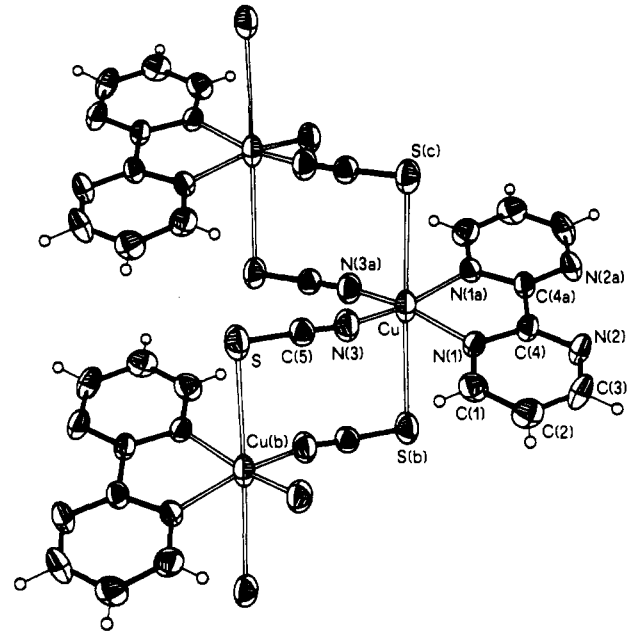

Figure 3. (a) ORTEP view of the $[Cu(bpm)(NCS)_2]_n$ complex (**2**) with the atom numbering scheme. Thermal ellipsoids are plotted at the 50% probability level. All hydrogen atoms are drawn with uniform isotropic thermal parameters.

bridged by two cyanato groups to different copper atoms at a distance of 5.921 Å. The cyanato compound grows in two directions (leading to a 2D-arrangement) by means of these bonds while the nitrate one grows only along one direction.

The Cu and Cu(a) atoms are at 0.108(1) Å up and down the N(1)N(2)C(2)C(2a)N(1a)N(2a) plane in the (NCO)Cu(bpm)-Cu(NCO) unit (the copper atoms are in the same plane for the corresponding chloride and bromide compounds),[10] whereas the N(3) and N(4) atoms are at –0.144(7) and –0.563(9) Å, respectively. Therefore, the geometry around copper atoms is more distorted than in the halogen Cu–bpm compounds. The Cu···Cu(a) (5.520(1) Å) and N(1)···N(2a) (2.371(5) Å) distances through the bipyrimidine bridge are practically identical to the corresponding ones in the $Cu_2(bpm)Cl_4$ compound (5.528(2) and 2.371(5) Å, respectively). Bond distances and angles in the bpm ligand are in the range of those reported previously for bis-chelating bipyrimidine-containing copper(II) complexes.[9,10]

The cyanato groups are quasi-linear (178.9(7) and 176.7(8)° for N(4)–C(5)–O(1) and N(3)–C(6)–O(2), respectively), and their C–O distances are longer than the C–N ones (C(6)–O(2) = 1.188(9) Å, C(5)–O(1) = 1.208(6) Å, N(3)–C(6) = 1.138(8) Å, and N(4)–C(5) = 1.145(6), Å). These structural features have been observed in other cyanato-bridged complexes with first-row transition metal ions.[12b,20] However, when cyanato bridges metal ions in a symmetrical end-on fashion, the difference between the C–N and C–O distances is significantly reduced.[21]

$[Cu(bpm)(NCS)_2]_n$ (2) and $[Cu_2(bpm)(NCS)_4]_n$ (3). The structure of complex **2** consists of neutral $Cu(bpm)(NCS)_2$ units which are bridged by sulfur atoms of the thiocyanate groups to yield a 1D-chain as shown in Figure 3. The arrangement of these chains in the unit cell running parallel to the z axis is illustrated by Figure 4. On the contrary, the structure of complex **3** is made up of neutral dinuclear $(NCS)_2Cu(bpm)Cu(NCS)_2$ units which are interconnected by thiocyanate groups acting in an end to end bridging fashion to yield a polymeric 3D-arrangement (Figures

(20) (a) Lloret, F.; Julve, M.; Faus, J.; Ruiz, R.; Castro, I.; Mollar, M.; Philoche-Levisalles, M. *Inorg. Chem.* **1992**, *31*, 784. (b) Duggan, D. M.; Hendrickson, D. N. *Inorg. Chem.* **1974**, *13*, 2056.

(21) (a) Kahn, O.; Mallah, T.; Gouteron, J.; Jeannin, S.; Jeannin, Y. *J. Chem. Soc., Dalton Trans.* **1989**, 1117. (b) Mallah, T.; Kahn, O.; Gouteron, J.; Jeannin, S.; Jeannin, Y.; O'Connor, C. J. *Inorg. Chem.* **1987**, *26*, 1375.

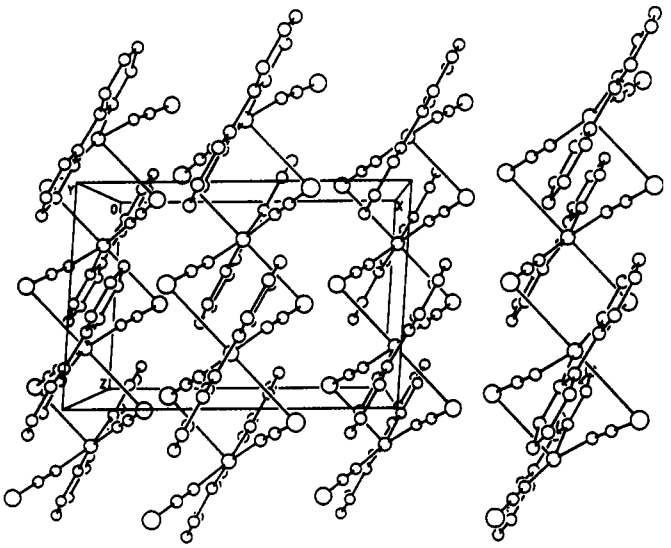

Figure 4. View of the crystal packing of complex **2** showing the arrangement of the 1D-chains running parallel to the *c*-axis (the *a*-axis is horizontal). Atoms are plotted with arbitrary atomic radii. Hydrogen atoms have been omitted for clarity.

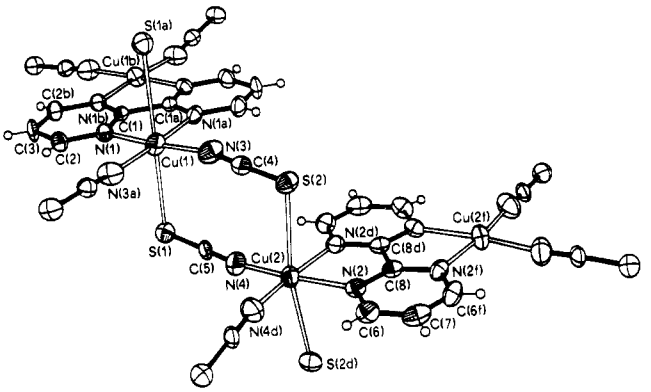

Figure 5. (a) ORTEP view of the $[Cu_2(bpm)(NCS)_4]_n$ complex (**3**) with the atom numbering scheme. Thermal ellipsoids are plotted at the 50% probability level. Shaded ellipsoids represent the atoms of the asymmetric unit. All hydrogen atoms are drawn with uniform isotropic thermal parameters.

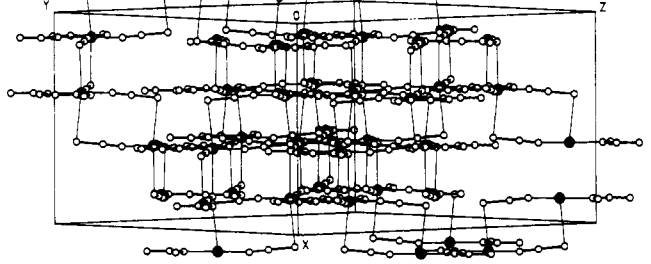

Figure 6. View of the cell of complex **3**. Atoms are plotted with arbitrary atomic radii. Dark circles denote the copper atoms. Hydrogen atoms have been omitted for clarity.

5 and 6). The copper atoms are, in both compounds, in a distorted octahedral surrounding with four nitrogen atoms in the basal plane, two from bipyrimidine and two from thiocyanate groups. Copper atoms are linked to each other through *S*-thiocyanate atoms, which are in trans positions, above and below the equatorial plane of the octahedron. In compound **3**, there are different $(NCS)_2Cu(bpm)Cu(NCS)_2$ units, which lie in parallel planes bridged by the same thiocyanate anions (Figure 5). The Cu–Cu axis, which joins copper atoms through the first bpm bridge, is perpendicular to the Cu–Cu axis of the second unit. Compound **3** grows along two directions, the Cu(1)–Cu(1a) axis being parallel to the *y* axis of the orthorhombic cell and the Cu(2)–Cu(2d) axis to the *z* one. The Cu–S bonds, which are approximately along the *x* axis, enable the growth along the third direction.

The Cu–NCS–Cu bonds in compound **2** form a zig-zag structure. This structure is similar, apart from the distortion around the copper atoms, to the observed one for the halogen complexes. However, the bis-bidentate coordination of bpm in the halogen compounds enables a 2D-arrangement, while the bidentate coordination of bpm in **2** leads to a 1D-chain. As far as the Cu–NCS–Cu bonds are concerned, the geometry in compound **3** is different. In fact, we can consider such a case, a helical arrangement around the Cu–NCS–Cu bonds, where the bpm molecules lie on parallel planes, and consequently, they turn around it. This is the substantial difference from **2** to **3**, apart the fact that bpm is bidentate in **2** and bis-bidentate in **3**. Consequence of this different behavior is the fact that compound **3** is a 3D-polymer, whereas it would be only a 2D-one, as in the halogen compounds, if the thiocyanate groups had been placed according to a zig-zag structure as in **2**.

Bond lengths and angles of the bis-bidentate bpm ligand in **3** are close to those reported for this ligand in other bipyrimidine-bridged complexes. Slight differences are observed when comparing with those of **2** which are most likely due to the fact that bpm is bidentate in this latter compound. The Cu–N bonds are shorter in **2** (2.009(6) Å) with respect to **3** (2.052(5) and 2.060(5) Å) and to **1** (2.072(4) Å). However, the substantial difference between **2** and **3** concerning the copper environment is the increase of the Cu–S distance (3.174(2) Å in **2**, compared to 2.947(1) and 2.932(1) Å in **3**). The lengthening of the Cu–S axial distance is related to a distortion towards a tetrahedral geometry in **2**, compared to **3**, as shown by a large distortion of the dihedral angle between N(3)CuN(3a) and N(1)N(1a)C(4a)C(4)N(2)N(2a)Cu mean planes (24.0(2)° in **2**; 1.2(2) and 1.1(2)° in **3**). A consequence of this distortion is the fact that the bpm separation in complex **2** (1.757(6) Å) is smaller than in **3** (3.203(1) Å). Both compounds **2** and **3**, become blue when the temperature is lowered. A similar behavior has been observed in other thiocyanate-containing metal complexes.[22] It was assumed that this thermochromism could be due to changes in the metal-thiocyanate bridging network when cooling down.

The Cu···Cu(b) distance is 5.328(2) Å in **2**, whereas the corresponding one in **3** (Cu(1)···Cu(2)), is 5.430(2) Å. Cu(1) and Cu(1b) atoms lie within the plane of the bridging bpm ligand (N(1)N(1a)C(1)C(1a)N(1b)N(1c)) in the first $(NCS)_2Cu(bpm)Cu(NCS)_2$ unit, whereas Cu(2) and Cu(2f) lie in the plane of the second one. The separation between copper atoms through the bpm bridge is the shortest found for this series of complexes (5.492(4) and 5.506(3) Å for Cu(1)···Cu(1b) and Cu(2)···Cu(2f), respectively).

The thiocyanato groups are almost linear in both complexes (179.6(7) and 178.2(6)° for N(3)–C(5)–S and N(4)–C(5)–S(1), respectively). The Cu–N–C(S) linkages are bent (165.0(6), 167.1(5), and 171.3(6)° for Cu–N(3)–C(5), Cu(1)–N(3)–C(4), and Cu(2)–N(4)–C(5), respectively). These structural features have been already observed in other thiocyanato-containing metal complexes.[23,24]

Infrared and Electronic Spectra. The most important aspects containing the infrared spectra of **1–3** deal with the possibility to distinguish between the chelating and bis-chelating coordination modes of bpm, and to characterize the presence of the different bridging modes of cyanate and thiocyanate. As far as the first point is concerned, a simple examination of Figure 7 reveals the

(22) Dockum, B. W.; Reiff, W. M. *Inorg. Chem.* **1982**, *21*, 1406.
(23) (a) McElearney, J. N.; Balagot, L. L.; Muir, J. A.; Spence, R. D. *Phys. Rev. B* **1979**, *19*, 306. (b) Cano, F. H.; García-Blanco, S.; Guerrero, Laverat, A. *Acta Crystallogr., Sect. B* **1976**, *32*, 1526. (c) Shevelashvili, M. A.; Porai-Koshits, M. A.; Antsyshkina, J. *Struct. Chem. USSR (Engl. Transl.)* **1969**, *10*, 552. (d) Nardelli, M.; Gasparri, A.; Musati, A.; Manfredotti, A. *Acta Crystallogr.* **1966**, *21*, 910. (e) Porai-Koshits, M. A.; Tishchenko, G. N. *Sov. Phys.-Crystallogr. (Engl. Transl.)* **1960**, *4*, 216.

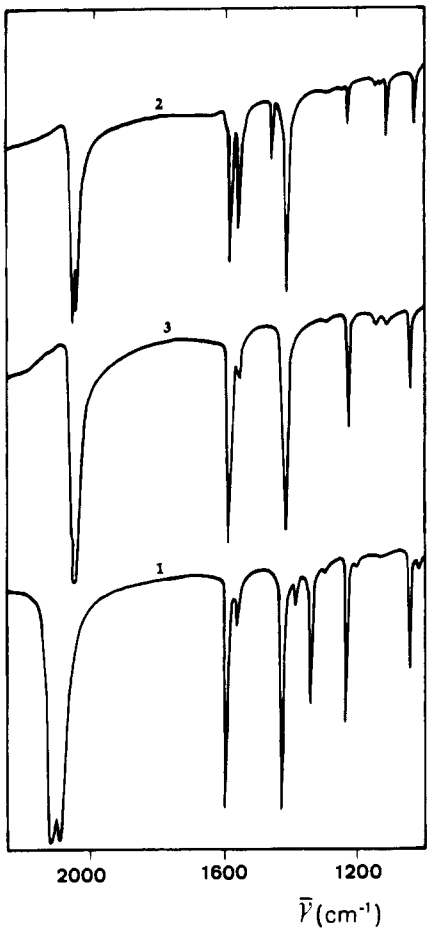

Figure 7. Infrared spectra of complexes **1**–**3** in the 2200–1000-cm^{-1} region.

presence of a strong absorption (ring stretching mode of bpm) as a quasi-symmetric doublet at ca. 1580 cm^{-1} in complex **2** (chelating bpm), whereas it appears as a very asymmetric doublet at identical frequency for complexes **1** and **3** (bis-chelating bpm). We observed these spectral features in other copper(II) complexes containing terminal[9,11a] and bridging bipyrimidine,[10] suggesting that the occurrence of a quasi-symmetrical or asymmetrical doublet in this region can be considered as diagnostic of bidentate or bis-bidentate bridging modes of bpm, respectively. Dealing with the second point, infrared criteria have been established to determine the coordination modes of cyanate and thiocyanate.[25] From these studies, it appears that the ν_{as}(NCX) stretching mode, located in the region near 2000 cm^{-1}, is very useful to determine the nature of the cyanate and thiocyanate coordination. In the present case, two bands are observed for the ν_{as}(N–C–X) vibration: 2230 and 2180 cm^{-1} for **1**, 2120 and 2100 cm^{-1} for **2**, and 2120 (sh) and 2100 cm^{-1} for **3**. Molecular symmetry requires doubling of the ν_{as}(NCX) vibration for all the tetrahedral and polymeric octahedral compounds, since the XCN–M–NCX group is not linear. These spectral features are in agreement with the 2D, 1D, and 3D arrangements of **1**, **2**, and **3**, respectively. In addition, the occurrence of the ν_s(NCO) stretching at 1340 (m) cm^{-1} for **1** supports the presence of end on cyanato bridge as confirmed by the crystallographic structure.

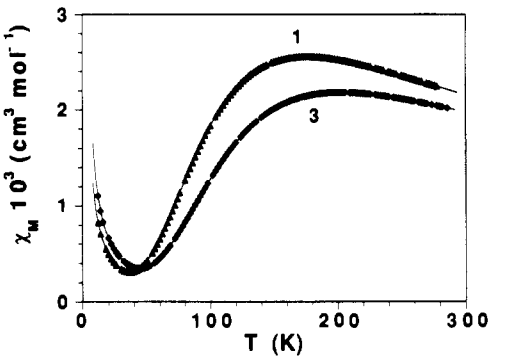

Figure 8. Thermal variation of the molar susceptibility (per dinuclear unit): exprimental points for **1** (▲) and **3** (◆) and theoretical (solid line) best fits.

The three complexes display similar electronic spectra. The high-energy region of the spectra of complexes **2** and **3** is characterized by the occurrence of intense charge transfer bands at 450 and 480 nm respectively, whereas this band is centered at 390 nm for complex **1**. The presence of two sulfur atoms in the coordination sphere of copper atoms in complexes **2** and **3** (CuN_4S_2 chromophore; CuN_4O_2 for **1**) accounts for this shifting toward higher wavelengths. Broad maxima centered at 690 (**1**), 660 (**2**), and 680 (**3**) nm are due to d–d transitions. Furthermore, a shoulder at 1100 nm is observed for complex **3**.

Magnetic Properties and EPR Spectra. The χ_M vs T curves for complexes **1** and **3** (χ_M being the molar susceptibility per dinuclear unit) are displayed in Figure 8, whereas the magnetic behavior of complex **2** is depicted in Figure 9 under the form of $\chi_M T$ (per mononuclear unit) vs T. The curves for complexes **1** and **3** exhibit smooth maxima at 165 and 197 K, respectively, and increases at low temperature due to the occurrence of uncoupled species. The $\chi_M T$ product for complex **2** decreases slowly at low temperature revealing a weak antiferromagnetic interaction between the copper(II) ions. The later data can be fitted with the empirical relation proposed by Estes et al.[26] for an antiferromagnetic 1D Heisenberg $S = {}^1/_2$ chains with

$$\hat{H} = -J\sum_{j=1}^{N-1}\hat{S}_i\cdot\hat{S}_{i+1} \qquad (1)$$

The susceptibility data of complexes **1** and **3** can be fitted by a simple Bleaney–Bowers dinuclear law, modified to include an amount of ρ% uncoupled species

$$\chi_M = 2N_A\beta^2g^2(1-\rho)/(kT(3+\exp(-J/kT))) + \rho C/T \qquad (2)$$

where J expresses the singlet-triplet energy gap and N_A, g, β, k, and T have their usual meaning. The best fit results are given in Table VIII. The results for complexes **1** and **3** are consistent with a large antiferromagnetic coupling through bpm bridge and a weak interaction between the $(XCN)_2Cu(bpm)Cu(NCX)_2$ units as observed in the parent nitrato, chloro, and bromo complexes.[10] Alternatively, we fitted the data of complexes **1** and **3** by the empirical expression proposed by Hatfield for alternating chains[27] or by a modification of the Bleaney–Bowers expression (3), taking

$$\chi_M = 2N_A\beta^2g^2(1-\rho)/[k(T-zJ')(3+\exp(-J/kT))] + \rho C/T \qquad (3)$$

into account the intermolecular interactions J' between z neighbors by means of a zJ' term in a molecular field approach. In any case, we found intramolecular J values for compounds **1** and **3**

(24) (a) Real, J. A.; De Munno, G.; Muñoz, M. C.; Julve, M. *Inorg. Chem.* **1991**, *30*, 2701. (b) Gallois, B.; Real, J. A.; Hauw, C.; Zarembowitch, J. *Inorg. Chem.* **1990**, *29*, 1152. (c) Antolini, L.; Fabretti, A. C.; Gatteschi, D.; Giusti, A.; Sessoli, R. *Inorg. Chem.* **1990**, *29*, 143. (d) Mukherjee, A. K.; Mukherjee, M.; Ray, S.; Ghosh, A.; Chaudhuri, N. R. *J. Chem. Soc., Dalton Trans.* **1990**, 2347. (e) Jide, X.; Shisheng, N.; Yujuan, L. *Inorg. Chem.* **1988**, *27*, 4651. (f) Real, J. A.; Zarembowitch, J.; Kahn, O.; Solans, X. *Inorg. Chem.* **1987**, *26*, 2939.

(25) (a) Bailey, R. A.; Kozak, S. L.; Michelson, T. W.; Mills, W. N. *Coord. Chem. Rev.* **1971**, *6*, 407. (b) Nelson, J.; Nelson, S. M. *J. Chem. Soc. A* **1969**, 1597. (c) Clark, R. J. H.; Williams, C. S. *Spectrochim. Acta* **1966**, *22*, 1081.

(26) Estes, W. E.; Gavel, D. P.; Hatfield, W. E.; Hodgson, D. J. *Inorg. Chem.* **1978**, *17*, 1415.

(27) Hatfield, W. E. *J. Appl. Phys.* **1981**, *52*, 1985.

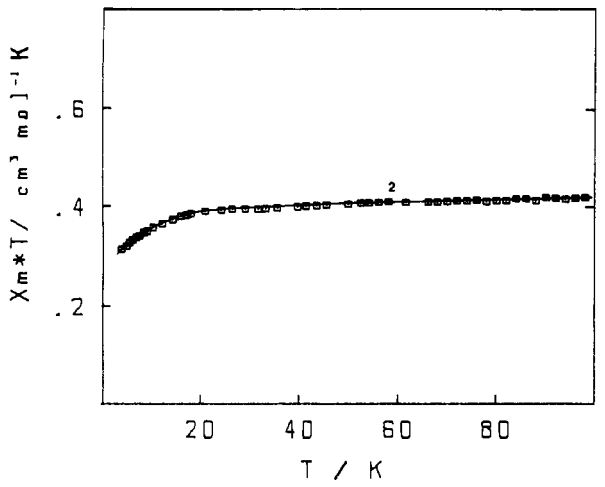

Figure 9. Thermal variation of the molar susceptibility per mononuclear unit of complex **2** in the form of $\chi_M T$ versus T: (⊡) experimental points; (—) best theoretical fit.

Table VIII. Best Fitted Values for J, g, and ρ

compd	$-J$, cm^{-1}	g	ρ, %	10^5R^a
1	199	2.19	1.1	3.0
2	0.6	2.06		2.8
3	230	2.17	1.5	3.2

^{a} R is the agreement factor defined as $R = \sum_i(\chi_{exptl}(i) - \chi_{calcd}(i))^2/\sum_i\chi_{exptl}(i)^2$.

significantly different from those obtained through expression 2, without significant improvement of the fits. These results strongly support our first hypothesis: the magnetic behavior of compounds **1** and **3** can be interpreted essentially within the dinuclear $(XCN)_2Cu(bpm)Cu(NCX)_2$ unit.

The X-band EPR spectra of complexes **1–3** recorded on microcrystalline powders show absorption features of axial symmetry ($g_\parallel = 2.275$ and $g_\perp = 2.091$ for **1**; $g_\parallel = 2.273$ and $g_\perp = 2.073$ for **2**; $g_\parallel = 2.285$ and $g_\perp = 2.080$ for **3**) whose intensities increase when cooling down from room temperature to 5 K. A weak half-field forbidden transition is observed at both room and low temperatures for all three compounds. The shape and thermal dependence of these signals suggest that they can be attributed to uncoupled copper(II) species. The occurrence of the $\Delta M_s = 2$ forbidden transition in **1–3** could be due to intermolecular interactions between the mononuclear copper(II) entities. We have already observed half-field forbidden transitions in well-characterized mononuclear copper(II) species.[28]

The aim of the present work was the synthesis of alternating copper(II) chains with J_i and J_{i+1} of different sign, that is, alternation of ferro and antiferromagnetic interactions. However, the coordination modes adopted by cyanato and thiocyanato bridges lead to antiferromagnetic coupling in 1D, 2D, and 3D networks. In the light of these results, three points deserve to be discussed: (i) the ability of bpm bridge to transmit antiferromagnetic interaction between copper(II) ions separated by about 5.5 Å; (ii) the influence of the structural parameters on the coupling constant J; and (iii) the bridging ligands to be used, other than cyanate and thiocyanate, in order to realize alternating ferro and antiferromagnetic exchange couplings.

(i) The strong antiferromagnetic coupling observed in **1** (−199 cm^{-1}) and **3** (−230 cm^{-1}) is of the same order of magnitude than those reported for the parent nitrato, chloro, and bromo bipyrimidine-containing copper(II) complexes.[10] For this family of complexes, extended Hückel calculations have shown that the strong antiferromagnetic interaction is due to the overlap of the d magnetic orbitals of d_{xy} symmetry centered on each copper(II) ion through the bpm bridge (σ in-plane overlap). An important energy gap (Δ) is obtained between the two singly occupied molecular orbitals which can be considered as the g and u combinations of the d_{xy} magnetic orbitals). In a series of complexes with similar geometry and when the ferromagnetic terms are negligible[29]

$$|J| \propto \Delta^2 \qquad (4)$$

and consequently, the larger the energy gap Δ, the greater the stabilization of the singlet state is.

(ii) The difference between the J values of **1** and **3** is small but beyond the limit of experimental errors. The structural data show that the bond distances and angles in the Cu(bpm)Cu units of **1** and **3** are similar. However, in **1**, the copper atoms are 0.108(1) Å above and below the bpm mean plane, whereas they are coplanar in **3**. The displacement of the metal ion toward the axial N(3b) atom in **1** is due to the stronger axial coordination in **1** (2.456(7) Å for Cu–N(3b)) with respect to **3** (2.947(1) and 2.933(1) Å for Cu(1)–S(1) and Cu(2)–S(2), respectively). Moreover, the bending angle γ (angle between bpm plane and the mean plane involving the basal donor set of atoms around copper), is 8.4° for **1** and 0.7° for **3**. Both factors, i.e. the displacement of the copper atom from the bpm plane and the greater γ value in **1**, lead to a lower $|J|$ value, compared to **3**. A similar result obtained for oxalato complexes was discussed recently.[30] In this context, it is satisfying that the parent isostructural compounds **1** and $[(NO_3)_2Cu(bpm)Cu(NO_3)_2]_n$[9,10] exhibit close exchange coupling values, −199 and −191 cm^{-1}, respectively.

As far as the intermolecular interactions between $(XCN)_2Cu(bpm)Cu(NCX)_2$ units are concerned, the structures of **1** and **3** exemplify two different situations: the end-on cyanato bridging in one dimension and the end to end cyanato bridging between the planar layers of stacked dinuclear units defining a second direction in the former complex and the end to end thiocyanato bridging between copper(II) ions of $Cu_2(bpm)$ units in the latter one.

Several observations lead us to conclude that weak intermolecular interactions are involved in **1** and **3**. First, the axial distances around copper in these compounds are long. If one chooses the Cu–Cu direction and the C–C inter ring bond as the x and y axes, respectively, the admixture of d_{z^2} orbitals (perpendicular to the xy plane) is small and the δ overlap between d_{xy} orbitals contained in $Cu_2(bpm)$ units separated by 2.21 Å through end-on cyanato and by 2.94 Å through end to end thiocyanato is expected to be small. Furthermore, the important slippage of the $Cu_2(bpm)$ units precludes a significant interaction. Second, the weak coupling observed in **2** is a rough estimation of the intermolecular interaction in **3**. Indeed, a very poor δ overlap between the d_{xy} magnetic orbitals is operative in **2** yielding to a very weak coupling. Third, no significant improvements of the fits and no significant changes of the J values were observed by treating magnetic data through the expression of alternating chains or a modified Bleaney–Bowers expression (vide supra).

(iii) Although the ability of pseudohalide ions to yield ferromagnetic coupling between copper(II) ions is well-known, their versatility as ligands made them unsuitable to build magnetic systems with regular alternation of ferro- and antiferromagnetic couplings under the conditions of the present paper. Simple ligands, such as hydroxo, could be more appropriate. In this regard, $Cu^{II}_2(OH)_2$ dinuclear units with CuOCu angles smaller than 97.5° are ferromagnetically coupled.[4,31] The triplet state is the low-lying state when 2,2′-bipyridine or 2,2′-bipyrimidine

(28) Julve, M.; Verdaguer, M.; Faus, J.; Tinti, F.; Moratal, M.; Monge, A.; Gutiérrez-Puebla, E. *Inorg. Chem.* **1987**, *26*, 3520.

(29) See e.g.: Daudey, J. P.; Gatteschi, D.; Hatfield, W. E.; Hendrickson, D. N.; Hodgson, D.; Kahn, O.; Solomon, A. A.; Whangho, M.; Willet, R. D. In ref 3.

(30) Alvarez, S.; Julve, M.; Verdaguer, M. *Inorg. Chem.* **1990**, *29*, 4500.

(31) Crawford, V. H.; Richardson, H. W.; Wasson, J. R.; Hodgson, D. J.; Hatfield, W. E. *Inorg. Chem.* **1976**, *15*, 2107.

are used as terminal ligands (L) in $[LCu(OH)_2CuL]^{2+}$ dinuclear units.[11a,32] Taking advantage of the bis-chelating character of the bypirimidine, one can use this dinuclear entity as a precursor of ···M(bpm)Cu(OH)$_2$Cu(bpm)M··· homo and polymetallic compounds which would exhibit regular alternation of ferro- and antiferromagnetic coupling.[33]

Acknowledgment. This work was partially supported by the Ministero dell' Università e della Ricerca Scientifica e Tecnologica (Italy), the Programa de Acciones Integradas Hispano-Francesas, and the Comisión Interministerial de Ciencia y Tecnología (Project PB88-0490) (Spain). The authors are most grateful to Professor P. Dapporto, University of Firenze for data collection for compound **3**.

Supplementary Material Available: Tables of crystallographic data (Table S1), anisotropic thermal parameters (Tables S2–S4), least-squares planes (Tables S5–S7), and nonessential bond distances and angles (Tables S8–S10) (12 pages). Ordering information is given on any current masthead page.

(32) (a) Toofan, M.; Boushehri, M.; Ul-Haque, M. *J. Chem. Soc., Dalton Trans.* **1976**, 217. (b) Majeste, R. J.; Meyers, E. A. *J. Phys. Chem.* **1970**, *74*, 3497. (c) McGregor, K. T.; Watkins, N. T.; Lewis, D. L.; Drake, R. F.; Hodgson, D. J.; Hatfield, W. E. *Inorg. Nucl. Chem. Lett.* **1973**, *9*, 423. (d) Casey, A. T.; Hoskins, B. F.; Whillans, F. D. *Chem. Commun.* **1970**, 904. (e) Hoskins, B. F.; Whillans, F. D. *J. Chem. Soc., Dalton Trans.* **1975**, 1267. (f) Barnes, J. A.; Hatfield, W. E.; Hodgson, D. J. *J. Chem. Soc., Chem. Commun.* **1970**, 1593. (g) McGregor, K. T.; Hodgson, D. J.; Hatfield, W. E. *Inorg. Chem.* **1973**, *12*, 731. (h) Barnes, J. A.; Hodgson, D. J.; Hatfield, W. E. *Inorg. Chem.* **1972**, *11*, 144. (i) Castro, I.; Faus, J.; Julve, M.; Verdaguer, M.; Monge, A.; Gutiérrez-Puebla, E. *Inorg. Chim. Acta* **1990**, *170*, 251. (j) Sletten, J.; Sørensen, A.; Julve, M.; Journaux, Y. *Inorg. Chem.* **1990**, *29*, 5054. (k) Castro, I.; Faus, J.; Julve, M.; Bois, C.; Real, J. A.; Lloret, F. *J. Chem. Soc., Dalton Trans.* **1992**, 47.

(33) De Munno, G.; Julve, M.; Lloret, F.; Faus, J.; Verdaguer, M.; Caneschi, A. Submitted for publication in *Angew. Chem.*